Organic Electronics 13 (2012) 1463–1469

Contents lists available at SciVerse ScienceDirect

Organic Electronics

journal homepage: www.elsevier.com/locate/orgel

Waveguided random lasing in red-emitting-dye-doped organic–inorganic hybrid polymer thin films

Luis Cerdán *, Angel Costela, Inmaculada García-Moreno

Instituto de Química Física "Rocasolano" (CSIC), Serrano 119, 28006 Madrid, Spain

ARTICLE INFO

Article history:
Received 31 January 2012
Received in revised form 11 April 2012
Accepted 22 April 2012
Available online 5 May 2012

Keywords:
Hybrid polymer
Waveguides
Dye lasers
Energy transfer
Random lasing

ABSTRACT

Long-wavelength (660–740 nm) coherent random lasing (RL) in slab waveguides consisting of poly(2-hydroxyethyl methacrylate) (pHEMA) incorporating silsesquioxane nanoparticles (POSS) doped with the red-emitting dyes LDS722 and LDS730 is presented. Energy transfer from a donor dye is used to overcome the inherent low pump (532 nm) absorption of these dyes and to enhance the lasing efficiency of the samples. Rhodamine 6G is used as donor for LDS722 and Sulforhodamine B as donor for LDS730, in donor/acceptor molar proportions 3.3/6.6 and 1/9, respectively. RL emission spectral fingerprints and thresholds are studied in depth and insights into the RL characteristics are obtained from the Power Fourier Transforms of the emission spectra. Finally, photostabilities of LDS722 and, for the first time, of LDS730 doped into polymer slab waveguides are assessed.

1. Introduction

Over the last few years laser scientists have been exploring the development of wave guiding structures based on organic materials since they are promising candidates for future applications in integrated photonics [1–5]. These materials, either organic semiconductors or dye-doped polymers, exhibit wide wavelength tunability and high efficiency, which combined with their potentially very low cost makes them attractive candidates for their exploitation as compact and versatile laser systems.

Most of the work on organic thin film lasers has been carried out with dyes emitting in the green–yellow spectral region [1–5], and few results have been published on thin film devices emitting in the deep red part of the visible spectrum (660–740 nm), even though this spectral region is of interest in biophotonic applications. Leaving apart specifically synthesized dyes, commercial dyes such as Rhodamine 640 [6], Nile Blue [7] and Oxazine 725 [8] have been used as dopants for active polymer waveguides with emission in the red. Surprisingly, well known hemicyanine dyes, which emit in the deep red spectral region [9,10] and are characterized by very broad absorption and emission bands and huge Stokes shifts [11], have not received much attention in this context.

On the other hand, it has been demonstrated [12–14] that active waveguides with high surface roughness due to phase separation in polymer blends may sustain waveguided coherent random lasing (RL), paving the way to the development of integrated devices technologically and economically more favorable that the ones based on nanopatterning (distributed feedback, Bragg reflectors, etc.).

In previous papers [12,14] we demonstrated that the presence of nanometer-sized particles based on polyhedral oligomeric silsesquioxanes (POSS) in dye-doped polymer slab waveguides could result in coherent RL due to the scattering induced by the high surface roughness coming from the polymer/POSS phase separation obtained after solvent evaporation. With the aim to obtain RL emission into the red spectral edge (660–730 nm), in the present work we have followed the same approach than the one described in Ref. [14], but using this time the commercial

* Corresponding author. Tel.: +34 915619400; fax: +34 915642431.
E-mail addresses: lcerdan@iqfr.csic.es (L. Cerdán), acostela@iqfr.csic.es (A. Costela), iqrfm84@iqfr.csic.es (I. García-Moreno).

1566-1199/$ - see front matter © 2012 Elsevier B.V. All rights reserved.
http://dx.doi.org/10.1016/j.orgel.2012.04.017

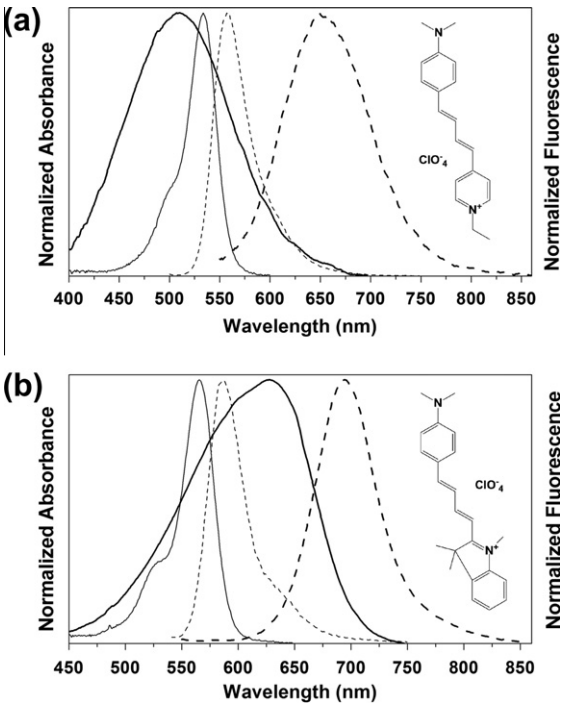

Fig. 1. Absorbance (solid lines) and fluorescence (dashed lines) spectral overlap of (a) Rh6G (thin lines)/LDS722 (thick lines) and (b) SRhB (thin lines)/LDS730 (thick lines), respectively. Insets show molecular structure of LDS722 and LDS730.

dyes LDS722 (also known as Pyridin 2) and LDS730 (also known as Styryl 6), which are charge transfer dyes belonging to the hemicyanine family with emission covering this spectral range (Fig. 1). It has been shown before [10,11] that LDS722 may sustain efficient and tunable DFB laser emission, but there are no reports of LDS730 being used in waveguide laser devices so far, which makes the results on LDS730 here presented a very novelty of the present work.

In this paper we report RL emission spectral fingerprints, thresholds and, for the first time, photostabilities from red-emitting dyes (LDS722 and LDS730) incorporated into asymmetric slab optical waveguides based on pHEMA/8OH-POSS (25%) polymer blends. An energy transfer approach is used to increase the final device efficiency. Insights into the RL characteristics are obtained from the Power Fourier Transforms of the emission spectra.

2. Materials and methods

Dyes LDS722 and LDS730 were laser grade and purchased from Exciton. Polymer poly(2-hydroxyethyl methacrylate) (pHEMA) and octa(hydroxypropyldimethylsilyl)-POSS (8OH-POSS), purchased from Aldrich, were used as received. The polymer chosen as dye host was pHEMA because the HEMA monomer mimics ethanol, which is a solvent in which hemicyanine dyes, due to their polar character, exhibited high lasing efficiency [11,15]. The POSS compound 8OH-POSS, which is soluble in polar solvents, was chosen to match the polar nature of pHEMA.

pHEMA (75 wt.%; 50 mg/mL), 8OH-POSS (25 wt.%; 16,7 mg/mL), and dye (10 mM with respect to the polymer) were added to ethanol and stirred for 24 h to fully solve dye and polymer. Increasing the amount of 8OH-POSS above 25% in weight resulted in the excess of 8OH-POSS being exuded from the sample. Films 1 m thick were obtained by spin coating (1000 rpm, 30 s) the polymer solution onto quartz substrates and left at room temperature for several minutes to remove the remaining solvent. We have found no way to measure directly the refractive index of the hybrid matrix since the film surface is rough and this leads to errors when using, for example, variable angle spectroscopic ellipsometry (VASE). We have estimated it taking into account that the refractive index of pHEMA is 1.51, and the one of 8OH-POSS is close to this value, as we have shown previously [16]. Then, the mixture of both must have a refractive index ~1.51. As this refractive index is higher than that of the quartz substrate (n = 1.456), the prepared samples defined asymmetric slab optical waveguides, where total internal refraction confines and guides the light along the film.

The absorbance and front face fluorescence spectra of the dye doped thin films were measured with a diode array spectrograph (Analytik Jena SPECORD 600) and a spectrofluorimeter (HORIBA Jobin Yvon Fluoromax-4), respectively.

The thin film samples were optically pumped at 532 nm with 20 ns full width at half maximum (FWHM) pulses from a frequency-doubled Q-switched Nd:YAG laser, operated at 15 Hz repetition rate. The pump radiation was vertically polarized, which allowed controlling the pulse energy incident on the sample by insertion into the pump beam path of a half-wave plate (HWP) and a linear polarizer (LP) set with its polarization axis vertical. By rotating the HWP the linear polarization of the input beam is rotated out of the vertical, and the pump beam is blocked more or less by the LP, depending on the rotation angle introduced by the HWP.

The light incident on the sample was perpendicular to the film surface and focused onto that surface in a stripe shape spot of ~150 microns width by a combination of negative and positive cylindrical quartz lenses (f = −15 and +15 cm, respectively), perpendicularly arranged. An adjustable slit was used to select only the central portion of the pump beam. Excitation stripes 2 mm long were defined, with an end placed right up to the edge of the film.

The RL emission was collected in the axis defined by the pumping stripe with a 5-cm focal length spherical lens, focused onto a fiber bundle and detected with a spectrograph/monochromator equipped with a thermoelectrically cooled CCD detector. Neutral density filters were used to avoid CCD detector saturation. The integration time in the CCD was set at 333 ms so that all the measurements were averaged over five pulses.

3. Results and discussion

We began the study by preparing samples doped with LDS722 (10 mM) alone and LDS730 (10 mM) alone. When these films were pumped at 380 kW/cm^2, RL was excited (Fig. 2a), but the emission was clearly weaker than that

obtained with sulforhodamines, partially due to the inherent lower efficiency and partially due to the lower absorption at 532 nm of LDS722 and LDS730 (Table 1). One approach to overcome the later is using mixtures of dyes in a system based on energy transfer, which is a physical phenomenon where excitation energy from an excited donor is radiatively (re-absorption/re-emission) and/or non-radiatively (Förster type via dipole–dipole coupling) transferred to a ground-state acceptor [20]. Thus, what is needed is a system consisting of two dyes, of which one (donor) should absorb efficiently the pump radiation at 532 nm and should be able to transfer the excitation energy to the second, low-absorbing long-wavelength emitting dye (acceptor). The energy transfer requires good overlap between donor emission and acceptor absorption bands, and depends strongly on the host medium and on the distance between donor and acceptor molecules. At the dye concentration used in this work (10 mM), the average intermolecular distance is approximately 7 nm, a value which is close to the typical Förster radius [20], meaning that the non-radiative transfer would be, a priori, efficient. Following this approach we tried Rhodamine 6G (Rh6G), Pyrromethene 567, Pyrromethene 597 and Sulforhodamine B (SRhB) as candidate donors for LDS722 and LDS730 due to the good overlap of their emission spectra with the absorption spectra of LDS722 and LDS730. We found that the best compromise between energy transfer and RL efficiency and photostability was obtained for the donor/acceptor pairs Rh6G/LDS722 and SRhB/LDS730. The good spectral overlap of the pairs Rh6G/LDS722 and SRhB/LDS730 can be appreciated in Fig. 1. The donor dyes by themselves exhibit good RL emission performance (efficiency and photostability, see Appendix A for Rh6G and Ref. [14] for SRhB) in their respective emission regions when placed alone into 8OH-POSS/pHEMA waveguides.

Table 1
Molar extinction coefficient at λ_{pump} (ε_A) and photoluminescence quantum yield (ϕ) of dyes used in this work.

	Rh6G	SRhB	LDS 722	LDS 730
ε_A (532 nm) [10^4 M^{-1} cm^{-1}]	7.7	2.6	2.3	1.4
ϕ	0.62[a]	0.61[b]	0.41[c]	0.59[b]

[a] Ref. [17].
[b] Ref. [18].
[c] Ref. [19].

The RL spectra from 1 m thin films with mixtures of Rh6G/LDS722 and SRhB/LDS730 in different molar proportions are shown in Fig. 2b and c, respectively. The highest output intensity (Fig. 2d and e) and collapse in the full width half maximum (FWHM) of the emission was obtained with mixtures of Rh6G/LDS722 in molar proportion 3.3/6.6 and SRhB/LDS730 in molar proportion 1/9. From now on every time we refer to samples Rh6G/LDS722 and SRhB/LDS730 it should be understood that the relative dye proportions are the optimal (3.3/6.6) and (1/9), respectively. The RL spectra from Rh6G/LDS722 and SRhB/LDS730 is overall much less collapsed that the RL spectra from Rh6G and SRhB alone. Although this could be a result of the lower efficiency of the formers, it is worth noticing that

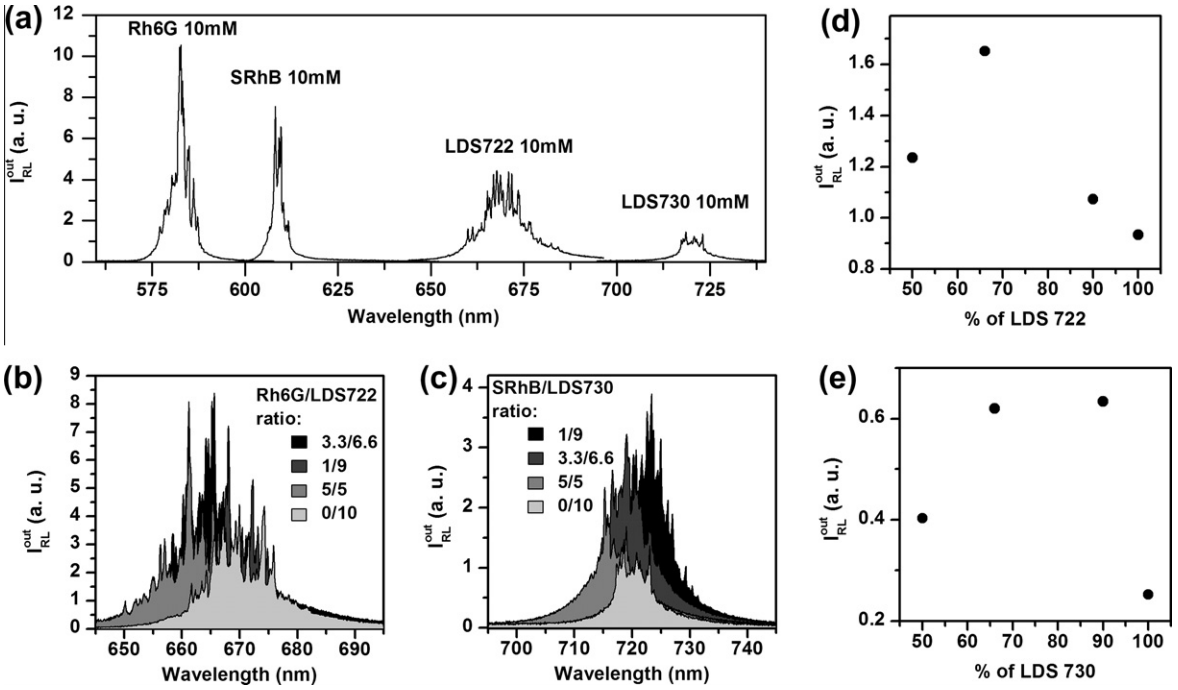

Fig. 2. RL emission spectra from waveguides based on pHEMA/8OH-POSS(25%) pumped at I_{pump} = 380 kW/cm^2: (a) doped with donor and acceptor dyes alone, (b) as a function of donor/acceptor molar ratio for the pair Rh6G/LDS722, and (c) as a function of donor/acceptor molar ratio for the pair SRhB/LDS730, (d) and (e) RL output intensity integrated over the whole spectral range as a function of percentage of LDS 722 and LDS 730, respectively.

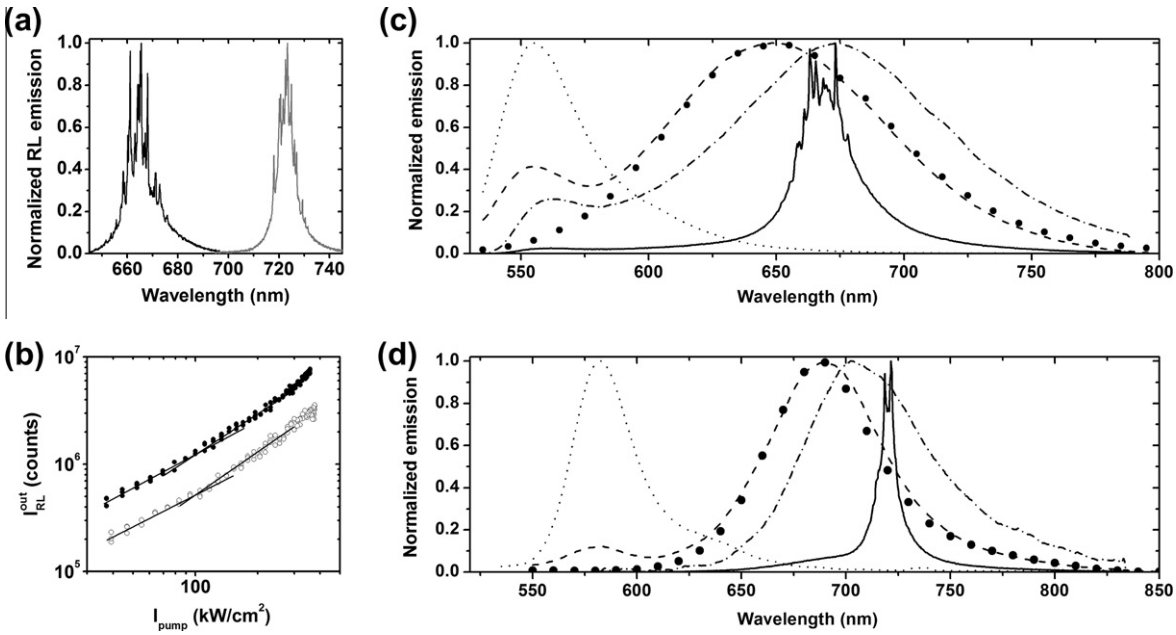

Fig. 3. RL and fluorescence measurements from waveguides based on pHEMA/8OH-POSS(25%): (a) Normalized RL output spectra at I_{pump} = 380 kW/cm^2 from samples Rh6G/LDS722 (black line) and SRhB/LDS730 (gray line). (b) RL output intensity (integrated over all wavelengths) as a function of pump intensity in the samples Rh6G/LDS722 (filled circles) and SRhB/LDS730 (hollow circles). Solid lines are a guide to the eye. (c) Front-face fluorescence (λ_{exc} = 532 nm) from samples doped with Rh6G 3.3 mM (dotted line), LDS722 6.6 mM (thick dots), Rh6G/LDS722 (3.3/6.6) 10 mM (dashed line) and fluorescence in RL set up at 30 kW/cm^2 in sample Rh6G/LDS722 (3.3/6.6) 10 mM (dash-dotted line) as compared with RL emission at 380 kW/cm^2 (solid line) of the last. (d) Front-face fluorescence (λ_{exc} = 532 nm) from samples doped with SRhB 1 mM (dotted line), LDS730 9 mM (thick dots), SRhB/LDS730 (1/9) 10 mM (dashed line) and fluorescence in RL set up at 30 kW/cm^2 in sample SRhB/LDS730 (1/9) 10 mM (dash-dotted line) as compared with RL emission at 380 kW/cm^2 (solid line) of the last.

the fluorescence FWHM (Fig. 1) of LDS722 and LDS730 reaches 100 and 63 nm, respectively, against the 41 and 37 nm of Rh6G and SRhB, respectively. In view of this fact, it could be concluded that the degree of collapse was greater in the hemicyanines (LDS722 and LDS730) than in the xanthenes (Rh6G and SRhB).

Fig. 3a shows the normalized RL emission spectra of the samples Rh6G/LDS722 and SRhB/LDS730, pumped at 380 kW/cm^2 with an excitation stripe of 2 mm. Both spectra exhibit a narrow ASE centered around 665 nm (Rh6G/LDS722) and 725 nm (LDS730) with very narrow peaks on top of it, with a linewidth smaller than 0.3 nm. As we had already concluded [14] the RL emission in the samples with 8OH-POSS originates in closed-loop random cavities formed in the medium due to the scattering induced by the high surface roughness coming from the pHEMA/8OH-POSS phase separation. Then, the waveguiding structure confines and guides the light, and the scattering feedback is obtained in the direction defined by the pumping stripe and the waveguide plane, with the emission consisting of overlapped RL and waveguide modes [21].

In Fig. 3b it is represented the dependence of the output intensity integrated over the whole spectrum with the pump intensity for both dyes. The estimated RL thresholds were in both cases close to 100 kW/cm^2, somewhat higher than the ones in the samples with Rh6G (60 kW/cm^2) and SRhB (50 kW/cm^2) alone. It is worth noticing at this point that the sample Rh6G/LDS722 presented some residual emission from Rh6G in the whole range of pump intensities used, meaning that the energy transfer was not complete. It is as well true that the residual emission from Rh6G was reduced as the pump intensity increased, indicating that there is a non-vanishing contribution of radiative transfer [20] to the overall energy transfer process. Nevertheless, the close proximity (~7 nm) and the good spectral overlap of donor and acceptor molecules (Fig. 1) suggest that non-radiative (FRET) energy transfer should have an important contribution to the overall energy transfer.

In order to estimate the weight of the FRET on the overall energy transfer in these donor/acceptor systems we had to minimize at maximum the effects of the radiative transfer processes. The steady-state front face measurement helps to minimize these processes since it reduces the optical path within the active medium, although it cannot remove them completely, since there will be always some optical path. As has been shown before [22], to reduce significantly the re-absorption/re-emission phenomena in these measurements, the optical path must be as short as possible. In the present samples the optical path in the front face measurement is determined by the sample thickness (~1 μm), which is short enough, less than two emitted wavelengths, as to minimize to a large extent the reabsorption/reemission effects, even at the high concentrations used in this work. In fact, we have compared the fluorescence emission obtained in the RL set-up at

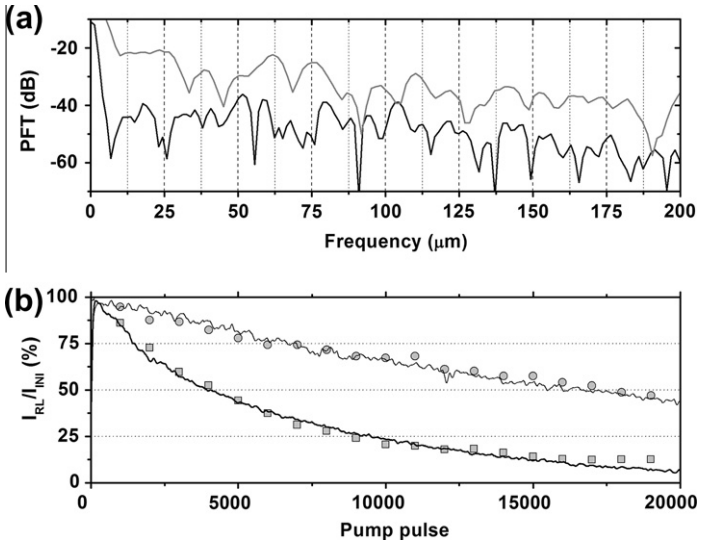

Fig. 4. (a) Power Fourier Transform (PFT) in decibels of RL spectra shown in Fig. 3a (Rh6G/LDS722 in black line and SRhB/LDS730 in gray line). (b) Evolution of the RL emission normalized to the first shot intensity as a function of the number of pump pulses in the same position for samples doped with Rh6G/LDS722 10 mM (filled squares), SRhB/LDS730 10 mM (filled circles), LDS722 10 mM (thick line) and LDS730 10 mM (thin line). Pump intensity and repetition rate were 550 kW cm^{-2} and 15 Hz, respectively.

the lowest pump intensity (30 kW/cm^2), in which the radiative transfer effects are enhanced due to the long optical path (2 mm), and the fluorescence (excited at 532 nm to compare the results with the RL measurements) in front-face configuration. The presence of homo radiative transfer (both from donor to donor and from acceptor to acceptor) should result in a red-shift of donor and acceptor emission peaks with respect to its fluorescence band, whereas the presence of hetero radiative transfer (from donor to acceptor) should result in a lower donor emission. It can be seen in the Fig. 3c and d that these two different radiative effects are minimized in the front-face fluorescence since the emission peaks are blue-shifted with respect to the RL set-up fluorescence and the donor emission is enhanced.

Fig. 3c and d show the fluorescence spectra of the donor alone, the acceptor alone and of the optimized mixtures from the pairs Rh6G/LDS722 and SRhB/LDS730, respectively. It can be observed in Fig. 3c that the energy transfer is not complete in the sample Rh6G/LDS722, since its spectrum clearly shows the band corresponding to the emission of Rh6G. On the contrary, the energy transfer is more favorable in the pair SRhB/LDS730, since the emission corresponding to SRhB is nearly negligible (Fig. 3d). It is possible to obtain an estimation of the FRET processes efficiency from the spectra shown in Fig. 3c and d. The FRET quantum yield ϕ_{FRET} is given by [20]:

$$\phi_{FRET} = 1 - \frac{I_F^{D+A}(\lambda_D^{peak})}{I_F^{D}(\lambda_D^{peak})}, \qquad (1)$$

where $I_F^{D+A}(\lambda_D^{peak})$ and $I_F^{D}(\lambda_D^{peak})$ are the fluorescence intensity at the donor emission peak in the presence and absence of acceptors, respectively. According to Eq. (1) and to the spectra shown in Fig. 3c and d (without normalization), it is found $\phi_{FRET}^{Rh6G/LDS722} \leqslant 0.9$ and $\phi_{FRET}^{SRhB/LDS730} \leqslant 0.98$. It is worth noticing that these values may be affected somewhat by radiative processes, and thus we have presented an upper-limit ($\leqslant$) instead of a full equality (=). Nevertheless, in the RL measurements the radiative transfer processes are activated thanks to the length traveled by the photons in the active medium and by the population inversion situation, which is translated into a less pronounced contribution of the donor emission to the final spectra, as can be observed as well in Fig. 3c and d. Whereas the sample SRhB/LDS730 shows no evidence of donor emission in its RL spectrum (Fig. 3d), the sample Rh6G/LDS722 still presents some contribution of the emission from Rh6G (Fig. 3c), as has been already mentioned. Then, the energy transfer in these systems is dominated by FRET and is reinforced by radiative transfer processes. As a final remark, time-resolved studies would provide more accurate information on the FRET phenomenon, but these measurements are beyond the scope of this work.

It is possible to gain insight into the excited random cavities by calculating the Power Fourier Transform (PFT) of the emission spectra. As it is well known, the PFT of the emission spectrum (in $k = 2\pi/\lambda$ space) from a well-defined laser cavity exhibits peaks at Fourier components with frequency $p_m = mL_C n/\pi$, where m is the order of the Fourier harmonic, L_C is the cavity path length, and n is the refractive index of the gain medium [23]. Fig. 4a shows the calculated PFT spectra of the emission spectra shown in Fig. 3a. The cavity path lengths resulted to be 21 and 23 μm for Rh6G/LDS722 and SRhB/LDS730, respectively. These path lengths are much longer than the waveguide thickness, meaning that, as expected, the feedback is taking place in the waveguide plane. The slight difference in the path length between the two samples can be ascribed to differences in the sample roughness, which changes along the sample and from sample to sample, and to the fact that the resonant conditions depend on the spectral

range, which is different in the samples Rh6G/LDS722 and SRhB/LDS730.

From a practical point of view, an important parameter in the behavior of the waveguides is the stability of the emission under long time operation, which implies high resistance to dye degradation under repeated pumping. It is worth noticing that, as far as we know, no photostability measurements have been performed on waveguides doped with LDS730. We assessed this stability by pumping the samples at a fixed position with a pump intensity of 550 kW/cm^2 (five times over RL threshold) and a repetition rate of 15 Hz. The actual evolution of the output emission integrated over a window of 10 nm around the emission peak is presented in Fig. 4b for both Rh6G/LDS722 and SRhB/LDS730. It can be observed that the RL emission decreased to 50% of the initial intensity after 4300 pump pulses in the sample Rh6G/LDS722 and after 18,000 pump pulses in the sample SRhB/LDS730. Then, SRhB/LDS730 is much more photostable that Rh6G/LDS722, fact that has been previously observed in bulk materials [15]. In Ref. [24] a much longer durability for LDS 722 was reported, with the emission falling to half of its initial value after 45,000 shots, instead of the 4300 measured in the present work. However, to properly compare both results it is necessary to consider the experimental conditions selected to carry out each particular experiment, since factors such as dye concentration, pump repetition rate, pump configuration and pump energy strongly affect the devices life-time. In fact, the particular thin film DFB laser presented in Ref. [24] had a thickness of 5 μm and a dye concentration of up to 38 mM, and was pumped at 160 μJ (267 kW/cm^2). Our thin film random laser has a thickness of 1 μm, a dye concentration of 10 mM and was pumped, for the photostability measurements, at 550 kW/cm^2. On the one hand, both a thicker film and a higher dye concentration may increase the measured photostability since, after all, there are more dye molecules to be destroyed. This effect is nicely reproduced in Fig. 4 of Ref. [24]. On the other hand, the lower the pump intensity is, the lower the degradation rate becomes. Then, with a thicker film, a higher concentration and a lower pump intensity the device in Ref. [24] was operated in better conditions to obtain a longer durability than our device. Therefore, once the experimental conditions are considered, the durability of our samples is not as short as could initially appear. Finally, to assess the effect that the energy transfer process might have on the devices operational lifetime, we measured the photostability of samples of LDS722 (10 mM) and LDS730 (10 mM) without donor, and found that the photostabilities of the samples with and without donor molecules were the same (Fig. 4b). This result suggests that the photostability of the mixture is limited by the intrinsic higher photodegradation rate of the emitting dye, which means that the improvement in the photostability should come from chemical modifications of dye, host or both.

4. Conclusions

We have studied in depth RL emission from red-emitting dyes (LDS722 and LDS730) incorporated into asymmetric slab optical waveguides based on pHEMA/8OH-POSS (25%) polymer blends. To circumvent the inherent low absorption of these dyes we have made use of energy transfer processes, both FRET and radiative transfer, by using mixtures of LDS722 with Rh6G and LDS730 with SRhB in donor/acceptor proportions 3.3/6.6 and 1/9, respectively. In the absence of time-resolved measurements, the fluorescence spectra study helps estimate that the FRET process reaches efficiencies of $\phi_{FRET}^{Rh6G/LDS722} \leqslant 0.9$ and $\phi_{FRET}^{SRhB/LDS730} \leqslant 0.98$. The sample with Rh6G/LDS722 gave RL emission centered at 665 nm whereas the emission from the sample SRhB/LDS730 was centered at 725 nm, both systems presenting a threshold close to 100 kW/cm^2. By calculating the Power Fourier Transform of the emission spectra the path length of the random cavities was estimated to be $L_C = 21$ m when the dye was Rh6G/LDS722 and $L_C = 23$ μm when the active medium was based on SRhB/LDS730. In both cases, the path length was much longer than the waveguide thickness, meaning that, as expected, the feedback is taking place in the waveguide plane.

Finally, we have measured the photostability of Rh6G/LDS722 and, for the first time, of SRhB/LDS730 in polymer waveguides, and have observed that the RL emission decreased to 50% of the initial intensity after 4300 pump pulses in the sample Rh6G/LDS722 and after 18,000 pump pulses in the sample SRhB/LDS730 when pumped at intensities five times above threshold.

In conclusion, it is possible to obtain efficient and photostable laser emission from dye-doped thin films in the deep red spectral range (660–730 nm) without the need of using complicated and expensive nanopatterned structures by incorporating in the polymeric material appropriate nanoparticles which induce structural changes.

Acknowledgments

This work was supported by projects MAT2010-20646-C04-01 and TRACE2009-0144 of the Spanish Ministerio de Economía y Competitividad (MINECO). L.C. thanks MINECO for a predoctoral scholarship (FPI, cofinanced by Fondo Social Europeo). We would like to thank the reviewers for their careful reading of the manuscript, which has allowed us to improve it significantly.

Appendix A. RL measurements from waveguides based on pHEMA/8OH-POSS (25%) doped with Rh6G

Fig. A1 shows the results on RL measurements from Rh6G (10 mM) doped waveguides. The RL emission was centered at 582 nm (Fig. A1a), characteristic of Rh6G, and had the threshold at 60 kW/cm^2 (Fig. A1b). From the spectrum shown in Fig. A1a a cavity path length of 23 μm was calculated (Fig. A1c). Photostability measurements were performed in this sample, and we found that the RL emission decreased to 50% of the initial intensity after 4700 pump pulses when pumped in a fixed position at 550 kW/cm^2 (ten times over RL threshold) with a repetition rate of 15 Hz.

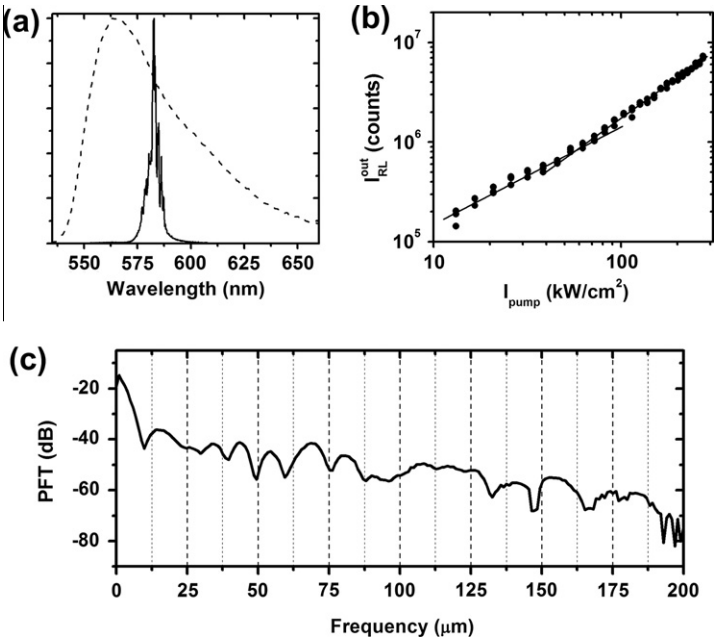

Fig. A1. RL results from Rh6G 10 mM doped pHEMA/8OH-POSS(25%) waveguides: (a) normalized fluorescence (dashed line) and RL output spectra at I_{pump} = 380 kW/cm^2 (solid line). (b) RL output intensity (integrated over all wavelengths) as a function of pump intensity. Solid line is a guide to the eye. (c) Power Fourier Transform (PFT) in decibels of RL spectrum shown in (a).

References

[1] E.M. Calzado, P.G. Boj, M.A. Díaz García, Amplified spontaneous emission properties of semiconducting organic materials, Int. J. Mol. Sci. 11 (2010) 2546–2565.

[2] S. Chénais, S. Forget, Recent advances in solid-state organic lasers, Polym. Int. DOI: http://dx.doi.org/10.1002/pi.3173.

[3] A. Costela, O. García, L. Cerdán, I. García-Moreno, R. Sastre, Amplified spontaneous emission and optical gain measurements from pyrromethene 567-doped polymer waveguides and quasi-waveguides, Opt. Express 16 (2008) 7023–7036.

[4] L. Cerdán, A. Costela, I. García-Moreno, O. García, R. Sastre, Waveguides and quasi-waveguides based on pyrromethene 597-doped poly(methyl methacrylate), Appl. Phys. B 97 (2009) 73–83.

[5] L. Cerdan, A. Costela, I. García-Moreno, O. García, R. Sastre, M. Calle, D. Muñoz, J. de Abajo, High-gain long-lived amplified spontaneous emission from dye-doped fluorinated polyimide planar waveguides, Macromol. Chem. Phys. 210 (2009) 1624–1631.

[6] S.S. Yap, W.O. Siew, T.T. Tou, S.W. Ng, Red-green-blue laser emission from dye-doped poly(vinyl alcohol) films, Appl. Opt. 41 (2002) 1725–1728.

[7] C.J. Oton, D. Navarro-Urrios, N.E. Capuj, M. Ghulinyan, L. Pavesi, S. González-Pérez, F. Lahoz, I.R. Martín, Optical gain in dye-impregnated oxidized porous silicon waveguides, Appl. Phys. Lett. 89 (2006) 011107.

[8] C. Ye, J. Wang, L. Shi, D. Lo, Polarization and threshold energy variation of distributed feedback lasing of oxazine dye in zirconia waveguides and in solutions, Appl. Phys. B 78 (2004) 189–194.

[9] Y. Oki, S. Miyamoto, M. Maeda, N.J. Vasa, Multiwavelength distributed-feedback dye laser array and its application to spectroscopy, Opt. Lett. 27 (2002) 1220–1222.

[10] Y. Oki, S. Miyamoto, M. Tanaka, D. Zuo, M. Maeda, Long lifetime and high repetition rate operation from distributed feedback plastic waveguide dye lasers, Opt. Commun. 214 (2002) 277–283.

[11] U. Beckmann, Lambdachorme Laser Dyes, first ed., Lambda Physik AG, Göttingen, 2000.

[12] L. Cerdán, A. Costela, I. García-Moreno, O. García, R. Sastre, Laser emission from mirrorless waveguides based on photosensitized polymers incorporating POSS, Opt. Express 18 (2010) 10247–10256.

[13] X. Zhao, Z. Wu, S. Ning, S. Liang, D. Wang, X. Hou, Random lasing from granular surface of waveguide with blends of PS and PMMA, Opt. Express 19 (2011) 16126–16131.

[14] L. Cerdán, A. Costela, G. Durán-Sampedro, I. García-Moreno, Random lasing from polymer slab waveguides doped with sulforhodamine dyes, Submitted elsewhere.

[15] I. García-Moreno, A. Costela, V. Martín, M. Pintado-Sierra, R. Sastre, Materials for a reliable solid-state dye laser at the red spectral edge, Adv. Funct. Mater. 19 (2009) 2547–2552.

[16] R. Sastre, V. Martín, L. Garrido, J.L. Chiara, B. Trastoy, O. García, A. Costela, I. García-Moreno, Dye-doped polyhedral oligomeric silsesquioxane (POSS)-modified polymeric matrices for highly efficient and photostable solid-state lasers, Adv. Funct. Mater. 20 (2009) 3307–3316.

[17] F. López-Arbeloa, T. López-Arbeloa, I. López-Arbeloa, A. Costela, I. García-Moreno, J.M. Figuera, F. Amat-Guerri, R. Sastre, Relations between photophysical and lasing properties of rhodamines in solid polymeric matrices, Appl. Phys. B 64 (1997) 651–657.

[18] I. López-Arbeloa, Private communication.

[19] L. Cerdán, A. Costela, I. García-Moreno, J. Bañuelos, I. López-Arbeloa, Singular laser behavior of hemicyanine dyes: unsurpassed efficiency and finely structured spectrum in the near-IR region, Laser. Phys. Lett. http://dx.doi.org/10.1002/lapl.2012.100.19.

[20] J.R. Lakowicz, Principles of Fluorescence Spectroscopy, Kluwer Academic/Plenum Publishers, New York, 1999.

[21] S. Kéna-Cohen, P.N. Stavrinou, D.D.C. Bradley, S.A. Maier, Random lasing in low molecular weight organic thin films, Appl. Phys. Lett. 99 (2011) 041114.

[22] I. López-Arbeloa, Fluorescence quantum yield evaluation: corrections for re-absorption and re-emission, J. Photochem. 14 (1980) 97–105.

[23] R.C. Polson, G. Levina, Z.V. Vardeny, Spectral analysis of polymer microring lasers, Appl. Phys. Lett. 76 (2000) 3858–3860.

[24] Y. Oki, K. Aso, D. Zuo, N.J. Vasa, M. Maeda, Wide-wavelength-range operation of a distributed-feedback dye laser with a plastic waveguide, Jpn. J. Appl. Phys. 41 (2002) 6370–6374.